Journal of Korean Association of Crystal Growth
Vol. 8, No. 4 (1998) 581-586

Relative quantitative evaluation of mechanical damage layer by X-ray diffuse scattering in silicon wafer surface

Chi-Young Choi and Sang-Hee Cho

Department of Inorganic Materials Engineering, Kyungpook National University, Taegu 702-701, Korea

실리콘 웨이퍼 표면에서 X-선 산만산란에 의한 기계적 손상층의 상대 정량 평가

최치영, 조상희

경북대학교 무기재료공학과, 대구, 702-701

Abstract We investigated the effect of mechanical back side damage in Czochralski grown silicon wafer. The intensity of mechanical damage was evaluated by minority carrier recombination lifetime by laser excitation/ microwave reflection photoconductivity decay method, degree of X-ray diffuse scattering, X-ray section topography, and wet oxidation/preferential etching methods. The data indicate that the higher the mechanical damage intensity, the lower the minority carrier lifetime, and the magnitude of diffuse scattering and X-ray excess intensity increased proportionally, and it was at Grade 1:Grade 2:Grade 3 = 1:7:18.4 that the normalized relative quantization ratio of excess intensity in damaged wafer was calculated, which are normalized to the excess intensity from sample Grade 1.

요 약 초크랄스키 실리콘 기판의 뒷면에 형성된 기계적 손상이 미치는 효과에 대하여 고찰하였다. 기계적 손상의 정도는 레이저 여기/극초단파 반사 광전도 감쇠법에 의한 소수반송자 재결합 수명, X-선 산만 산란, X-선 단면 측정 및 습식 산화/선택적 식각 방법으로 평가하였다. 그 결과, 웨이퍼 뒷면에 가해지는 기계적 손상의 세기가 강할수록 소수반송자 재결합 수명은 짧아지고, 산만 산란 정도와 X-선 과잉 강도의 적분값은 비례적으로 증가하였으며, 그 값을 Grade 1의 손상된 웨이퍼에서의 과잉 강도로 정규화하면 과잉 강도의 상대 정량 비는 Grade 1:Grade 2:Grade 3 = 1:7:18.4이다.

1. Introduction

It has been reported [1, 2] that laser excitation/ microwave reflection photoconductivity decay (μ-PCD) method is a noncontact, nondestructive, and high throughput technique with higher sensitivity than secondary ion mass spectroscopy and total reflection X-ray fluorescence spectrometry from the metal contamination monitoring point of view. Also it is commonly recognized that minority carrier lifetime measured by the μ-PCD method is very sensitive to crystallographic defects which can act as trap centers [3]. The other technique is applicable to the monitoring of low-level lattice damage in the manufacturing processes of VLSI. That is, high resolution X-ray diffraction is a widely used technique that provides a lot of information such as crystalline quality, epitaxial structure, layer thickness, and composition, etc. Triple crystal X-ray diffractometry (TCD) especially offers a highly strain-sensitive technique since narrow rocking curves are strongly influenced by small rotations caused by strains in the crystal [4]. For an ideal perfect crystal, diffracted beam has appreciable intensity only in the immediate vicinity of Bragg peak. However, thermal vibration and structural disorders change the distribution of X-ray leading to diffuse X-ray scattering. Therefore, it is useful to examine polish-induced strain, surface damage, as well as the crystallinity by analyzing rocking curves and the diffuse scattering of X-ray beams since diffuse scattering can be explained as the result of defect clusters or dislocation loops. Most of the work on the diffuse scattering of X-rays has been concerned with defects in the bulk of the crystal, and the interest has recently focused on

obtaining information from near surface regions.

In silicon wafer industry, the mechanical damage method, which provides dislocation and/or stacking fault nuclei [5, 6] on wafer back side, is one of the extensively used extrinsic gettering techniques [7] since it is simple and less costly.

In this work, electrical and structural evaluations on the effect of mechanically damaged surface in Czochralski (CZ) silicon wafers were executed by μ-PCD method, X-ray diffuse scattering, X-ray section topography, and wet oxidation/preferential etching methods.

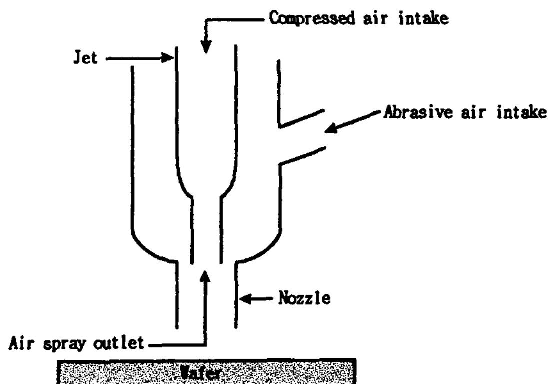

Fig. 1. Schematic of the liquid honing method.

2. Experimental

The starting material in this study was p-type (boron-doped, 9-20 Ω · cm) CZ silicon wafers of (100) with 200 mm diameters. The wafer was sliced along the (100) surface without an off angle, and then single-side polished to a thickness of 725 μm. The oxygen concentration measured with a Bio-RAD QS-300 FTIR according to the New ASTM procedure (ASTM F121-81 [8]) was 13.3~16.6 ppma, whereas the carbon level was less than 0.05 ppma which is below the detection limit of FTIR.

The wafers were heat treated at 700℃ for 10 min in N_2 ambient for oxygen donor annihilation [9] and each cleaved into quarter pieces. One piece from each wafer was not mechanically damaged. This piece was designated as the "Reference" to distinguish it from the second, the third and the fourth pieces, designated Grade 1, Grade 2, and Grade 3, whose back sides were mechanically damaged with three kinds of grades as shown in Table 1, respectively, using the liquid honing method (in Fig. 1).

After the liquid honing process, the samples were cleaned by RCA cleaning method and then subjected to surface passivation treatments, such as HF dipping for 10 min by high purity 49 % HF chemical of semiconductor grade and dry oxidation at 1000℃ for 40 min (the thickness of grown oxide layer is about 400 Å), to minimize the surface recombination velocity for lifetime measurements [10].

Table 1
Liquid honing process parameters

Grade	Air pressure* (kgf/cm^2)	Conveyer speed* (mm/sec)	No. of nozzle*
1	1	12.3	1
2	4.3	12.3	1
3	5.7	10	2

(*: normalized value).

The measurement of minority carrier recombination lifetime for the samples was performed at room temperature with a μ-PCD lifetime measurement system (SEMILAB WT-85X). The decay of excess minority carriers generated by irradiation with a pulsed laser beam (pulse width : 200 nsec, wavelength : 904 nm) impinged onto the polished surface is observed by monitoring the time decay of the microwave (10 GHz) reflection power since the conductivity decreases with the recombination of excited carriers, and accordingly the microwave reflection power decays.

The stresses on as-received wafers caused by mechanical damage were evaluated by employing a TCD (Bede diffractometer 300) and an X-ray topography system (Bede L6). In TCD analysis, X-ray diffraction with $\lambda = 1.5406$ Å of Cu $K\alpha_1$ radiation from a Rigaku D/MAX 2400 V rotating anode generator was used. The beam was conditioned by a four reflection, two crystal monochromator using grooved Si(111) crystals and was then allowed to strike the sample placed on the first axis of the diffractometer. Diffracted intensity from the sample crystals (004) reflection was analyzed by a grooved, three reflection (220) crystal situated on the second axis of the diffractometer. An X-ray generator power of 50 kV and 140 mA was used for the scan. For a diffuse scattering evaluation, the samples were scanned in the range of 400 arcsec with a 2 arcsec step interval. A full map of the scattering from the samples was made by recording the intensity from a series of separate sample and analyzer positions, which were coupled so as to trace a grid in reciprocal

space. Two-bounce and 4-bounce channel cut collimators were used as the beam conditioner and the beam analyzer, respectively. An X-ray section topography by Mo Kα_1 radiation was also used to observe the distribution of stress in the bulk. In order to reveal the defects generated as a result of relieving the stresses caused by the liquid honing method, the samples were oxidized at 1100℃ for 60 min in wet oxygen ambient and then inspected under the optical microscope after Wright etching [11] for 1 min.

3. Results and discussion

3.1. Relationship between mechanical damage intensity and lifetime

Figures 2(a) and 2(b) show minority carrier recombination lifetime data measured with μ-PCD technique in nondamaged ("Reference") and back side mechanically damaged silicon wafers. These data clearly show that the higher the mechanical damage intensity, the lower the minority carrier lifetime. It is well known that the actual penetration depth of laser beam (904 nm wavelength) into silicon crystal bulk is less than 30 μm [12].

However, as shown in Fig. 2, it is obvious that electrons and holes excited by laser beam are propagated up to wafer back side, consequently affecting the minority carrier recombination lifetime value. Judging from this, we can suggest that nondamaged wafers be used to obtain correct data for contamination and defect monitoring during device processing.

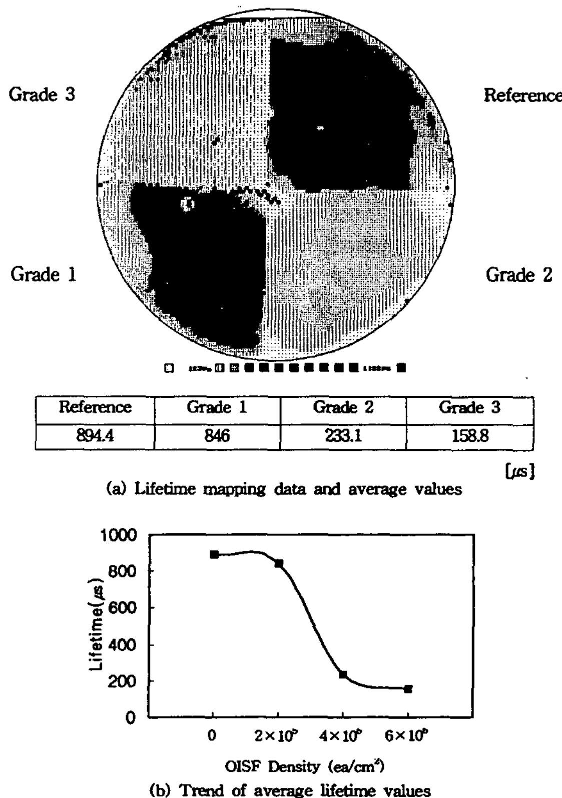

Reference	Grade 1	Grade 2	Grade 3
894.4	846	233.1	158.8

[μs]

(a) Lifetime mapping data and average values

(b) Trend of average lifetime values

Fig. 2. Relationship between the mechanical damage intensity and minority carrier recombination lifetime meaured by the μ-PCD technique. (a) Lifetime mapping data and average values and (b) Trend of average lifetime values.

3.2. Characterization of Stresses

To evaluate the stresses caused by the liquid honing method, we have performed X-ray diffuse scattering by TCD and X-ray section topography analyses. Figures 3(a)-3(d) show the reciprocal space map of (400) surface from a $\omega/2\theta$ scan by TCD as a function of mechanical damage grade. This reciprocal space map enables direct observation of diffuse scattering, which gives qualitative information of structural imperfections by mechanical damage. The diffuse scattering could be measured in this instance from the point $[q_y, q_z]$, which is related to the deviations of sample and the analyzer from their zero positions at the nominal Bragg angle. It is well known that the dynamical diffraction and surface streak are in the same direction for symmetric reflections, but the directions are not the same for asymmetric reflections, and the surface streak is always normal to the surface. The beam conditioner and the analyzer streaks are parallel to the Ewald sphere at the origin and at the hkl point, respectively. They are caused by finite angular collimation or resolution, allowing high intensities at the center of the plot to leak in these directions. However, the streaks can be reduced by multiple reflections in the beam conditioner and analyzer [13]. The TCD equipment that was used in this experiment has the four-bounce channel cut collimator in the beam analyzer for resolution improvement. Therefore, the analyzer streak will not show up in the reciprocal space map.

A horizontal simple scan across the map gives a

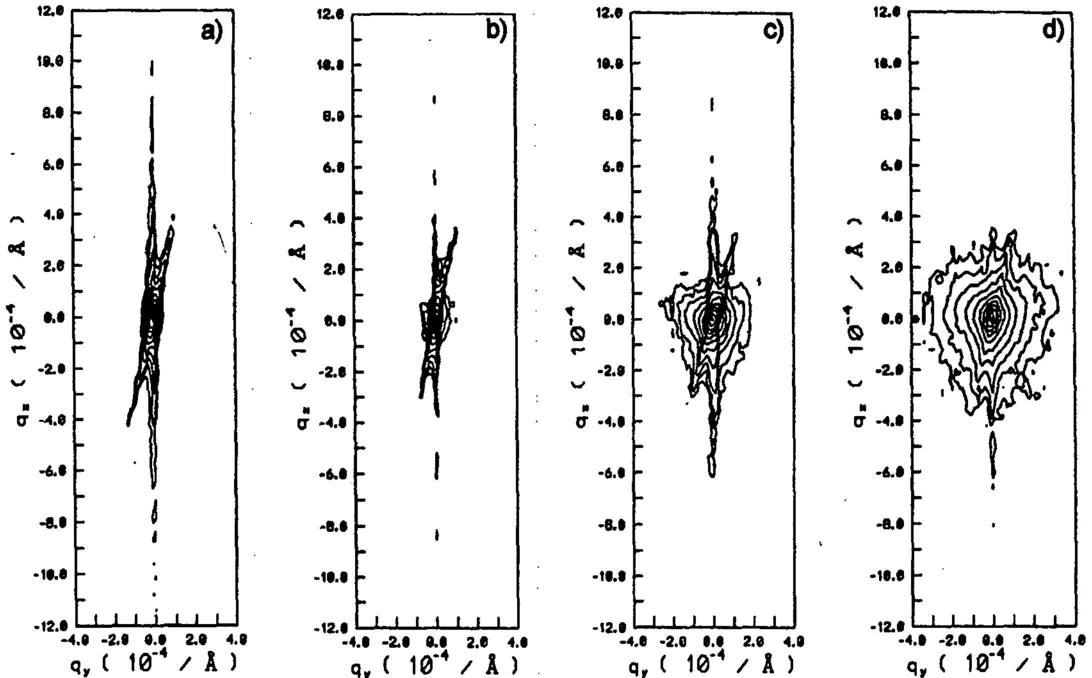

Fig. 3. Reciprocal space map with log intensity contour for the (a) Reference, (b) Grade 1, (c) Grade 2, (d) Grade 3. The contour distance is 0.4.

rocking curve with a fixed detector position. In the Reference sample shown in Fig. 3(a), only the isointensity contour from the dynamical diffraction and beam conditioner streak was shown without diffuse scattering; this signifies good quality crystal. As the grade of mechanical damage increased, a significant difference in the magnitude of diffuse scattering and its distribution in the reciprocal space map was observed. The dynamical streak disappeared gradually and the contour plot was getting wide, each of which indicated that the generation of imperfect near surface led to the increase of diffuse scattering. The diffuse scattering showed isotropic characteristics however.

Excess intensity, which is scattered intensity excluding the dynamical diffraction, was defined for a relative comparison and evaluation of diffuse scattering with respect to mechanical damage [14]. In equation (1), a total diffracted intensity is calculated by performing cylindrical integration from minimum and maximum values of $[q_y, q_z]$ that are equivalent to the whole volume of reciprocal space. From this point of view, excess intensity for a perfect silicon crystal such as the Reference sample will be zero, and the other samples of Grades 1, 2, and 3 were used for the calculation of the excess intensity. The resultant relative excess intensity for Grades 1, 2, and 3 showed 1, 7, 18.4 respectively, which are normalized to the intensity from sample Grade 1. These quantitative values signify the relative excess intensity of diffuse scattering so it is worth evaluating the degree of mechanical damage by the liquid honing method.

$$I_{excess} = \int_{-q_z}^{+q_z} \int_{q_{y,min}}^{q_{y,max}} I_n(q_y, q_z) dq_y dq_z \quad (1)$$

Figure 4 displays the stresses revealed by X-ray section topography technique with (440) reflection and Mo Kα_1. The Pendellösung fringes indicate high perfection of CZ silicon wafers used for this study. These data clearly indicate that the stresses even in Grade 1 of liquid honing method are propagated from mechanically damaged points on back side toward front surface to the extent of almost whole wafer thickness.

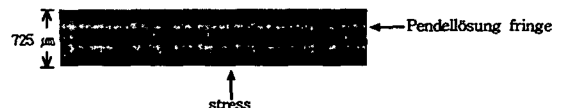

Fig. 4. The stress revealed by X-ray section topograph. [(440) reflection, Mo Kα_1].

The defects on the front side of the samples generated during wet oxidation at 1100℃ for 60 min as a result of relieving the stresses caused by the liquid honing method are shown in Fig. 5, and the data as follows; Grade 1 is 2×10^5 ea/cm^2, Grade 2 is 4×10^6 ea/cm^2, Grade 3 is 6×10^6 ea/cm^2 each. Note that the harder the mechanical damage intensity, the higher the oxidation induced stacking fault (OISF) density. It can be deduced that OISF test method would be a useful way to distinguish mechanical damage grades.

4. Conclusions

The stresses caused by mechanical damage and their effects were evaluated by minority carrier recombination lifetime by laser excitation/microwave reflection photoconductivity decay method, X-ray diffuse scattering, X-ray section topography, and

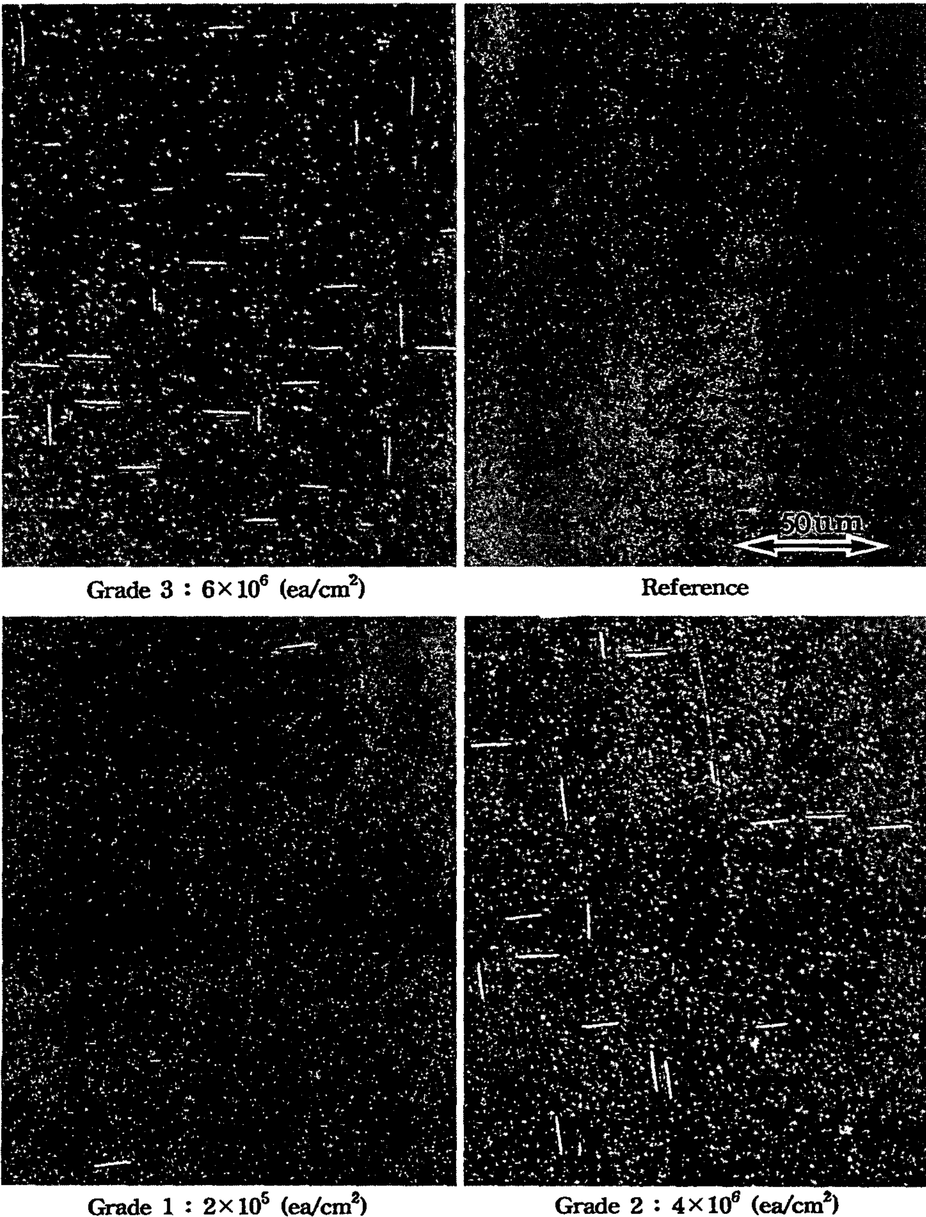

Fig. 5. Oxidation induced stacking faults generated during wet oxidation at 1100℃ for 60 min.

wet oxidation/preferential etching methods.

The results indicate that:

1) The higher the mechanical damage intensity, the lower the minority carrier recombination lifetime,

2) The degree of diffuse scattering increased proportionally, and the normalized relative quantization ratio of excess intensity is Grade 1: Grade 2:Grade 3 = 1:7:18.4, which are normalized to the excess intensity from sample Grade 1.

References

[1] A. Usami, Proc. IEEE 1991 Int. Conference on Microelectronic Test Structures 4 (1991) 1.

[2] A. Buczkowski, Z.J. Radzimski, G.A. Rozgonyi and F. Shimura, J. Appl. Phys. 72 (1992) 2873.

[3] K. Katayama, Y. Kirino, K. Iba and F. Shimura, Jpn. J. Appl. Phys. 30 (1991) L1907.

[4] B.K. Tanner and D.K. Bowen, J. Cryst. Growth 126 (1993) 1.

[5] M.L. Polignano, G.F. Cerofolini, H. Bender and C. Claeys, J. Appl. Phys. 64 (1988) 869.

[6] F. Shimura, Semiconductor silicon crystal technology, (Academic Press, Inc., San Diego, 1989) p. 350.

[7] S. Hahn, 1989 International Conference on VLSI and CAD, (KITE/IEEE Korea section) 238.

[8] Annual Book of ASTM Standards, F121-81, (American Society for Testing and Materials, Philadelphia, 1987).

[9] V. Cazcarra and P. Zunino, J. Appl. Phys. 51 (1980) 4206.

[10] D.K. Schroder, Semiconductor material and device characterization, (John Wiley & Sons, Inc., New York, 1990) p. 359.

[11] M.W. Jenkins, J. Electrochem. Soc. 124 (1977) 757.

[12] C. Fujihara, M. Morin, H. Hashizume, J. Friedt, Y. Nakai and M. Hirose, Jpn. J. Appl. Phys. 32 (1993) L1362.

[13] P. Zaumseil and U. Winter, Phys. Status Solidi A 70 (1982) 497.

[14] R.J. Matyi and B. Crist, Jr., J. Polym. Sci., Polym. Phys. Ed. 16 (1978) 1329.